Am J Transl Res 2025;17(11):8757-8766
www.ajtr.org /ISSN:1943-8141/AJTR0164654

Original Article

Regulation of ulcerative colitis progression by ferroptosis pathway genes: HSP90AA1, SNCA, TLR4, and PTGS2

Xueming Gai, Shiying Shen, Xiaoyun Sui, Kaiwen Liu

Department of Gastroenterology, Weifang Hospital of Traditional Chinese Medicine, Weifang 261000, Shandong, China

Received March 20, 2025; Accepted September 14, 2025; Epub November 15, 2025; Published November 30, 2025

Abstract: Objective: To investigate the role of the ferroptosis pathway in ulcerative colitis (UC) and conduct molecular validation. Methods: The UC dataset GSE3365 was downloaded from the GEO database, and differentially expressed genes were identified after data correction. Ferroptosis-related genes were obtained from the FerrDb database and intersected with the differentially expressed genes. Gene ontology (GO) and KEGG enrichment analyses were performed. A protein-protein interaction (PPI) network was constructed, leading to the identification of four hub genes. Thirty mice were randomly assigned to control, UC, and Ferrostatin-1, (Fer-1) groups (10 mice per group). UC was induced in the UC and Fer-1 groups using sodium dextran sulfate, and Fer-1, an iron death inhibitor, was injected into the Fer-1 group. Pathologic changes in colonic tissues were observed by H&E staining, serum TNF-α levels were measured with ELISA, and RT-qPCR was used to detect the expression of hub genes. Results: A total of 24 ferroptosis-related genes were identified in UC. GO enrichment analysis showed that these genes were involved in oxidative stress response, glucocorticoid response, and reactive oxygen species metabolism. PPI network analysis identified HSP90AA1, SNCA, TLR4, and PTGS2 as hub genes. Pathologic changes were alleviated in the Fer-1 group compared with the UC group. Serum TNF-α levels were significantly higher in the UC and Fer-1 groups than in the control group, with the UC group showing higher levels than the Fer-1 group (both $P<0.05$). The expression of HSP90AA1, SNCA, TLR4, and PTGS2 mRNA was significantly higher in UC and Fer-1 groups compared to the control group, with lower levels in the Fer-1 group than in the UC group (both $P<0.05$). Conclusions: HSP90AA1, SNCA, TLR4, and PTGS2 are ferroptosis-related genes that may play a crucial role in the pathogenesis of UC by regulating the ferroptosis pathway.

Keywords: Ferroptosis pathway, ulcerative colitis, gene expression analysis, validation experiments

Introduction

Ulcerative colitis (UC) is a chronic intestinal disease characterized by persistent inflammation of the colonic mucosa. The global incidence of UC is increasing annually, and it is listed by the World Health Organization among the refractory diseases [1, 2]. The pathogenesis of UC is complex, involving multiple factors such as genetic susceptibility, intestinal dysbiosis, immune system activation, and dysfunction of the intestinal mucosal barrier [3, 4]. Although the current treatment regimen, which h includes aminosalicylic acid preparations, glucocorticoids, and biological agents, can partially relieve clinical symptoms, approximately 30% of patients still exhibit poor responses to traditional treatments. Moreover, long-term use of these medications often leads to complications such as infections and metabolic disorders [5, 6]. Therefore, exploring the molecular mechanisms underlying UC and identifying new therapeutic targets has become a key area of research.

In recent years, there has been increasing interest in the role of programmed cell death in inflammatory diseases. Ferroptosis, a novel iron-dependent mode of cell death, is characterized by the accumulation of lipid peroxidation products and inactivation of the glutathione peroxidase system [7, 8]. Research has shown that ferroptosis is involved in the pathology of cancers and neurodegenerative diseases, and it is also closely linked to damage to the intestinal epithelial barrier in inflammatory bowel diseas-

https://doi.org/10.62347/WZRR7919

Table 1. Primer sequences

Primer	Sequence
HSP90AA1	5'-GACGCTCTCTGGATAAAATCCGTT-3'
	5'-TGGGAATGAGATTGATGTGCAG-3'
SNCA	5'-GGGAGTCCTCTATGTAGGTTCC-3'
	5'-TCCAACATTTGTCACTTGCTCT-3'
TLR4	5'-ATGGCATGGCTTACACCACC-3'
	5'-GAGGCCAATTTTGTCTCCACA-3'
PTG2	5'-AGCGTCAGGTCCCGTTTTC-3'
	5'-CTGGTGCATTGTGTTGGGT-3'
GAPDH	5'-AGCGTCAGGTCCCGTTTTC-3'
	5'-AGCGTCAGGTCCCGTTTTC-3'

es [9, 10]. Intestinal epithelial cells serve as the first line of defense against intestinal pathogens and are crucial for maintaining immune homeostasis. Abnormal cell death in these epithelial cells can lead to increased intestinal permeability and persistent inflammation. The oxidative stress mechanisms associated with ferroptosis may influence UC by regulating arachidonic acid metabolism, inflammatory factor release, and other signaling pathways [11, 12]. Studies have observed abnormal mitochondrial morphology and dysregulated expression of iron metabolism-related proteins in the colon tissues of UC patients, suggesting that ferroptosis may play a role in its pathogenesis. However, there is still a gap in research regarding the systematic identification of key regulatory genes involved in ferroptosis in UC and their molecular validation [13]. Building on previous findings, this study aims to characterize the expression patterns of ferroptosis-related genes in UC through bioinformatics and experimental validation, thereby elucidating the molecular regulatory network of ferroptosis in UC and providing a foundation for developing therapy targeting this pathway.

Materials and methods

Key genes in UC analyzed by GEO database

Data acquisition: Gene expression data from the GSE3365 dataset were downloaded from the GEO database (http://www.ncbi.nlm), including 85 enteritis samples and 42 control samples.

Data processing: Differentially expressed genes in the GSE3365 dataset were analyzed using the online tool (http://www.ncbi.nlm.nih.gov/geo/geo2r). The screening criteria were an adjusted *P*-value (adj. P) <0.05 and |logFC|≥ 1.5. A positive logFC indicates gene overexpression, while a negative logFC indicates underexpression.

UC and ferroptosis related genes: Ferroptosis-related genes were searched in the FerrDb database (http://zhounan.org/ferrdb/), including "Driver" and "Suppressor" genes. Differentially expressed genes from the previous analysis were intersected with ferroptosis-related genes. Intersections and Venn plots were generated using OmicStudio (http://www.omistudio.cn/tool).

Gene Ontology (GO) and Kyoto Encyclopedia of Gene and Genomes (KEGG) enrichment analysis: Filter conditions were set with *P*-value <0.05 and Q-value <0.05. GO and KEGG enrichment analyses of the intersecting genes were performed using the R package "clusterProfiler", with visualization of significant results using ggplot2.

Construction and module analysis of protein-protein interaction (PPI) network: A web-based PPI network for the intersecting genes was constructed using the STRING database (http://cn.string-db.org/cgi/input.pl) to visualize the data.

Consensus clustering analysis: The clustering analysis was conducted on the 24 intersecting genes in intestinal inflammation tissues using the ConsensusClusterPlus software package. The number of unsupervised clustering categories was quantitatively estimated with 50 iterations and an 80% resampling rate [14]. Principal component analysis was used to assess subtype differences.

Screening of hub genes: Cytoscape software, with the CytoHubba plugin, was used to analyze the topology of the PPI network. The top five node genes were identified and intersected as hub genes using three methods: "Degree", "MNC", and "EPC".

Verification by animal experiments

Experimental animals: Thirty healthy SPF-grade C57BL/6J mice, weighing 20 ± 2 g, were purchased from the Animal Experiment Center of Chongqing Medical University. The mice underwent a one-week fitness training period. Re-

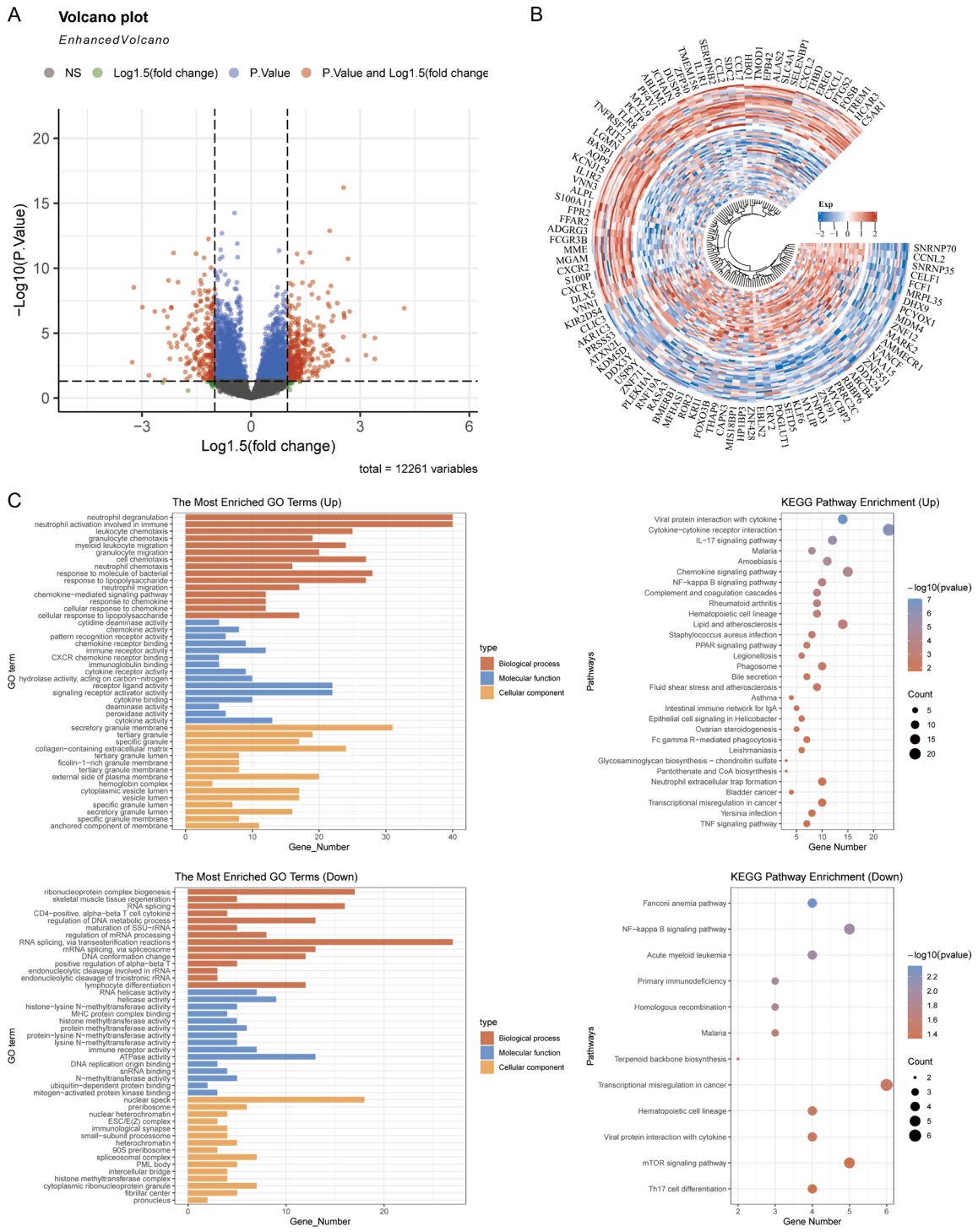

Figure 1. Differentially expressed genes and functional enrichment. A: Volcano plot of differentially expressed genes; B: Heat map of differentially expressed genes; C: GO term enrichment analysis and KEGG enrichment analysis of differentially expressed genes.

aring conditions included a temperature of 22-26°C, humidity of 40-70%, a 12-hour light-dark cycle, and free access to water and feed.

The study was approved by the Weifang Hospital of Traditional Chinese Medicine animal ethics committee.

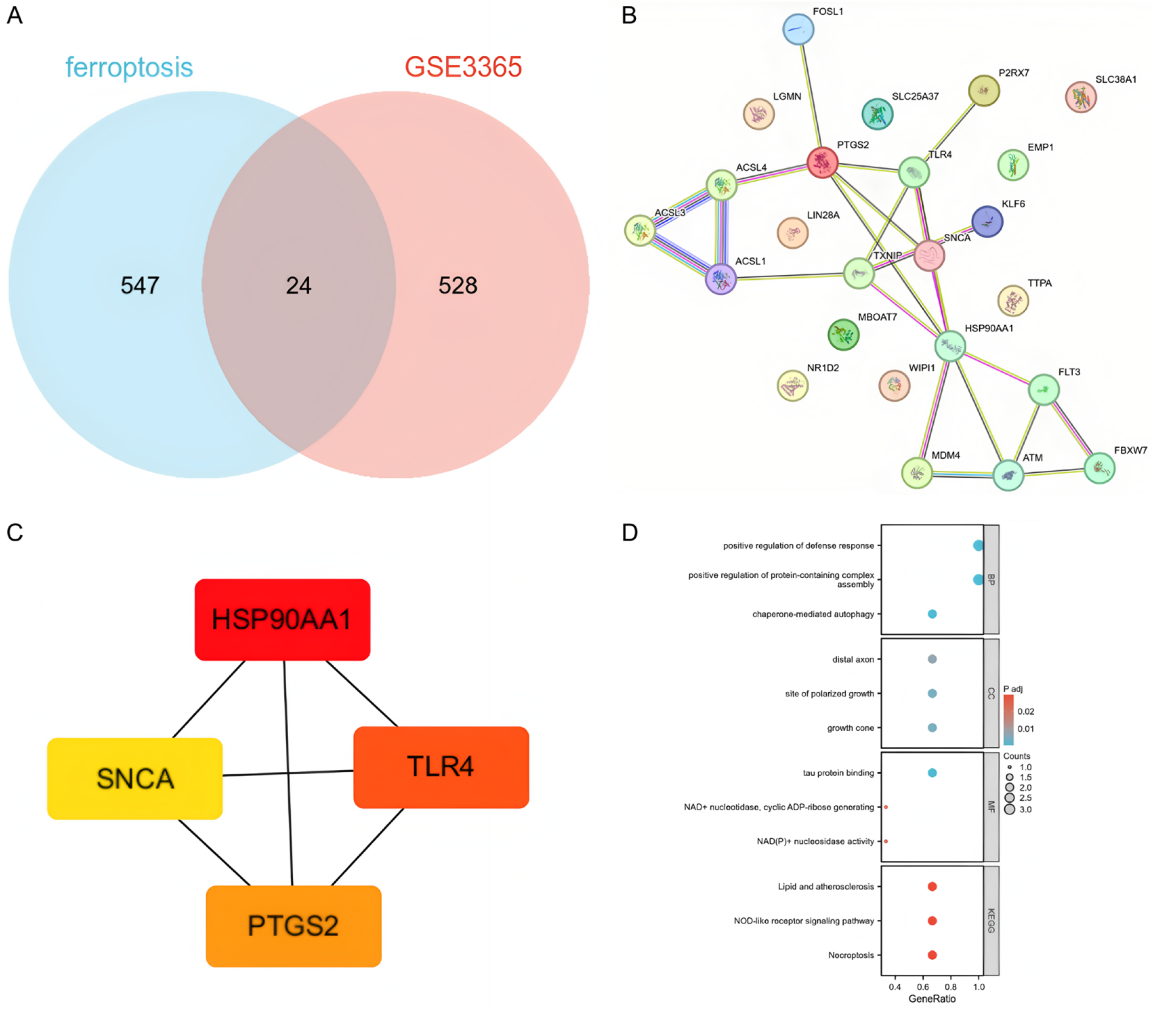

Figure 2. Hub gene screening. A: Venn diagram of intersection of the above differentially expressed genes and ferroptosis-related genes; B: Protein-protein interaction network diagram; C: Selected Hub genes; D: GOKEGG enrichment analysis of Hub genes.

Animal model: The mice were randomly divided into three groups (control, UC, and Fer-1) with 10 mice per group. UC modeling was performed with 3% dextran sulfate sodium (DSS, Sigma Corporation, USA) [15]. Fresh DSS solution was replaced daily. Successful modeling was indicated by the appearance of blood in stool on days 4 to 5. In the Fer-1 group, Fer-1 (Sigma, USA), an iron death inhibitor, was administered intraperitoneally at 10 mg/kg per day for 7 days starting from the first day of model establishment. Mice were euthanized by cervical dislocation after anesthesia with 4%-5% isoflurane.

H&E staining: H&E stain was performed to observe pathologic changes in colon tissues. Colonic mucosal tissues were fixed in 10% neutral formaldehyde, embedded, dehydrated, and sectioned. Stained slides were observed under a high-power microscope. Tissue inflammation was scored using the Gebobes system, with criteria ranging from 0 (no structural changes) to 5 (erosion or ulceration).

Detection of serum TNF-α, IL-1β, and IL-6 content: Whole blood (0.5 ml) was collected from each group using anticoagulation tubes, centrifuged and analyzed using ELISA kit (Abcam, USA) for TNF-α, IL-1β, and IL-6 levels.

Detection of oxidative stress markers in mouse serum: Blood samples (0.5 ml) were collected, centrifuged, and the serum analyzed for glutathione (GSH), malondialdehyde (MDA), and reactive oxygen species (ROS) levels using ELISA kits (Abcam, USA).

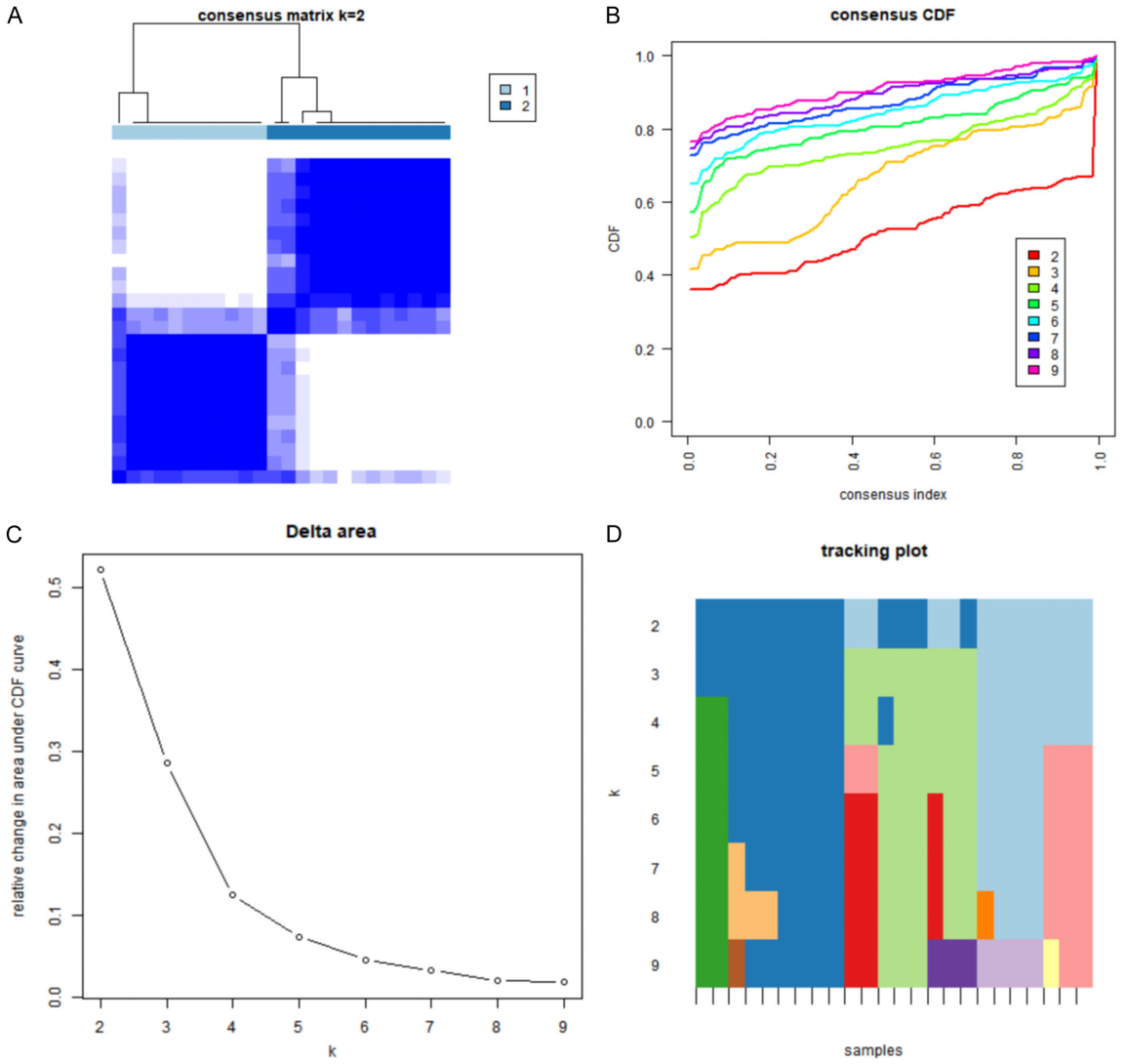

Figure 3. Construction of subtypes of enteritis tissues. A: Consensus matrix heatmap at k=2. B: CDF from k=2 to k=9. C: Relative changes in the area under the CDF curve. D: Sample classification tracking diagram from k=2 to k=9. CDF: Cumulative distribution function.

Identification of hub genes in colon tissues: Total RNA from colon tissues was extracted using TRIzol reagent (Invitrogen, USA) and reverse transcribed into cDNA. GAPDH was used as an internal reference gene. RT-qPCR was conducted with the following conditions: 95°C for 10 minutes, followed by 40 cycles of 95°C for 15 seconds and 60°C for 1 minute. Relative gene expression was calculated using the $2^{-\Delta\Delta Ct}$ method. Primer sequences are listed in **Table 1**.

Western blot detection of protein expression in mouse colon tissues: Proteins from colon tissues were extracted using a protein extraction kit (Shanghai Beyotime Biotechnology, China), and concentrations were determined using a BCA assay kit. A total of 20 μg of protein was separated by SDS-PAGE and transferred to PVDF membranes. After blocking with 5% skim milk, membranes were incubated overnight at 4°C with primary antibodies against HSP90AA1, SNCA, TLR4, and PTGS2 (Abcam, USA), followed by secondary antibody incubation. Images were developed using ECL chemiluminescence and analyzed with ImageJ software. β-actin served as the internal reference protein.

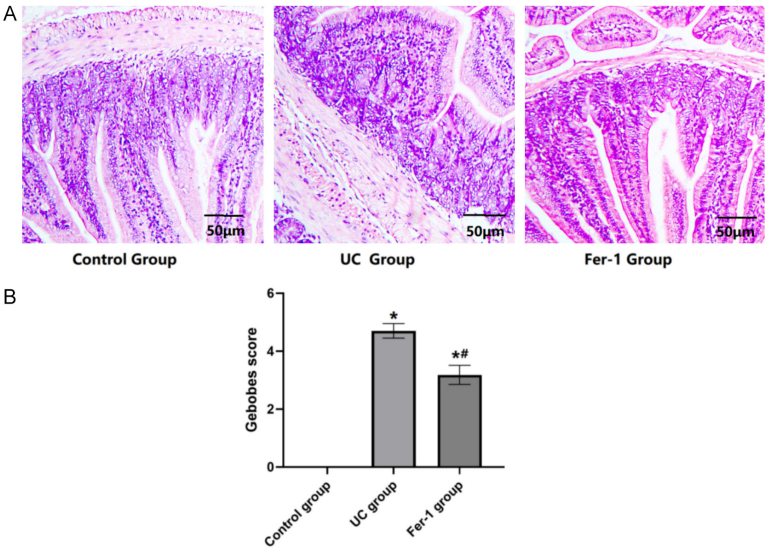

Figure 4. H&E staining and Gebobes score of colon in each group of mice. Note: (A) H&E stain of the colon in each group of mice (×400); (B) Gebobes score of each group of mice. Compared to the control group, *P<0.05; Compared to UC group, #P<0.05.

Statistical analysis

Statistical analysis was performed using SPSS 27.0. Continuous data were expressed as mean ± standard deviation ($\bar{x} \pm s$), and categorical data as counts and percentages. The t-test was used for comparisons of continuous data, and the χ^2 test for categorical data. One-way or two-way ANOVA followed by LSD testing was used for comparisons among multiple groups. A *P*-value <0.05 was considered significant.

Results

Differential gene expression in GSE3365 dataset

Analysis of the GSE3365 dataset revealed 571 differentially expressed genes, with 338 up-regulated and 233 down-regulated. Functional enrichment analysis was then performed on these genes, as shown in **Figure 1**.

Construction of intestinal inflammation tissue subtypes and screening of hub genes

The intersection of the differentially expressed genes and ferroptosis-related genes was analyzed, yielding 24 intersecting genes (**Figure 2**). A PPI network was constructed, and as shown in **Figure 3**, the optimal number of subtypes was determined to be 2. Principal component analysis results indicated complete separation between the two subtypes, with each being well-defined. Therefore, we classified the intestinal inflammation tissues into C1 and C2 subtypes based on the 24 intersecting genes. Using Cytoscape software, four hub genes were identified: HSP90AA1, SNCA, TLR4, and PTGS2.

Pathology of mice

Pathologic examination revealed that the colonic mucosa of control mice was smooth, with a well-organized glandular structure and normal crypts, without neutrophil infiltration, thickening, congestion, edema, or ulceration of the intestinal wall. In contrast, the UC and Fer-1 groups showed disrupted colonic mucosal tissue, disorganized glandular structures, crypt disappearance, obvious ulceration, and inflammatory cell infiltration. The UC group showed destruction of colonic mucosal tissue, disorganization of glandular structure, disappearance of crypts, obvious ulceration, and inflammatory cell infiltration. These pathologic changes were reduced in the Fer-1 group compared to the UC group. The Gebobes scores of the UC and Fer-1 groups were significantly higher than that of the control group (P<0.05), and the Gebobes score in the Fer-1 group was significantly lower than that in the UC group (P<0.05), as shown in **Figure 4**.

Comparison of Serum TNF-α, IL-1β, and IL-6 levels

Serum levels of TNF-α, IL-1β, and IL-6 were significantly higher in the UC and Fer-1 groups compared to the control group (all P<0.05). Additionally, the UC group exhibited significantly higher levels of these markers than the Fer-1 group (all P<0.05) (**Figure 5**).

Comparison of serum GSH, MDA, and ROS levels among mice groups

Serum GSH levels in the UC and Fer-1 groups were significantly lower than those of the con-

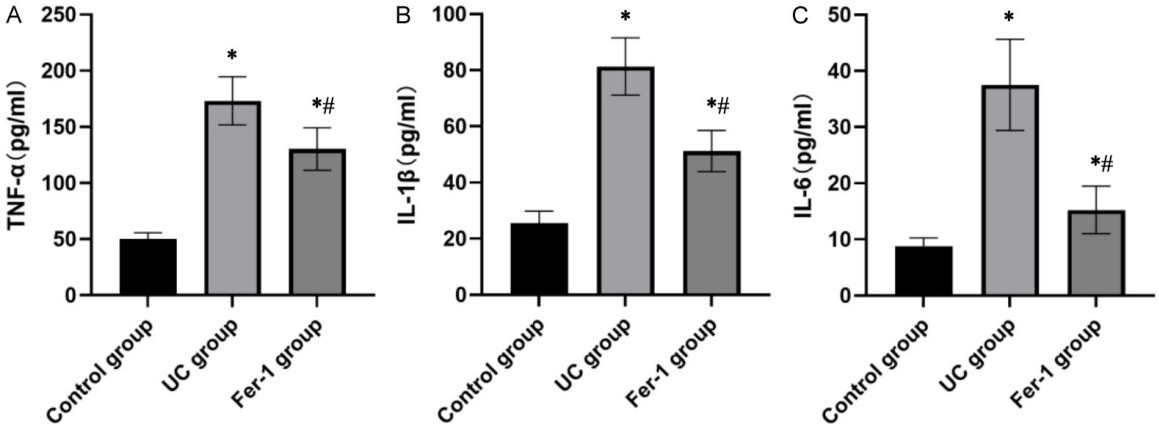

Figure 5. Comparison of serum TNF-α, IL-1β and IL-6 of mice in each group. Note: (A) TNF-α. (B) IL-1β. (C) IL-6. Compared to the control group, *P<0.05; Compared to UC group, #P<0.05. TNF-α: Tumor necrosis factor-α. IL-1β: Interleukin-1β. IL-6: Interleukin-6.

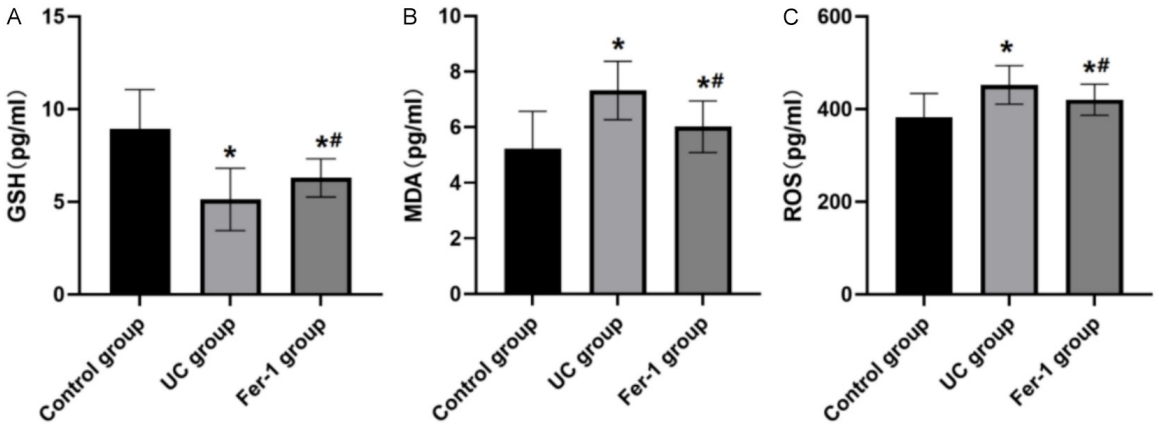

Figure 6. Serum GSH, MDA, and ROS levels in each group of mice. A: GSH. B: MDA. C: ROS. Compared to the control group, *P<0.05; Compared to UC group, #P<0.05. GSH: glutathione. MDA: Malondialdehyde. ROS: Reactive Oxygen Species.

trol group (P<0.05), while serum MDA and ROS levels were significantly higher (both P<0.05). GSH levels in the UC group were significantly lower than those in the Fer-1 group, and MDA and ROS levels were significantly higher in the UC group than in the Fer-1 group (all P<0.05, **Figure 6**).

Hub gene and protein expression in colonic tissues of each group

The relative mRNA expression levels of HSP-90AA1, SNCA, TLR4, and PTGS2, as well as their protein expressions in the colon tissues of the UC and Fer-1 groups, were significantly higher than those of the control group (all P<0.05). Notably, both the mRNA and protein levels of these hub genes in the Fer-1 group were lower than those of the UC group (all P<0.05, **Figure 7**).

Discussion

UC is a chronic inflammatory bowel disease characterized by complex interactions between genetic predisposition, immune dysfunction, intestinal microbiota imbalance, and oxidative stress [16-18]. In recent years, ferroptosis, a novel form of programmed cell death, has gained attention in inflammatory disease research due to its close association with lipid peroxidation and iron metabolism [19-21]. Key features of ferroptosis include inhibition of glutathione peroxidase, accumulation of ROS, and lipid peroxidation. These processes can exacerbate damage to the intestinal epithelial barrier

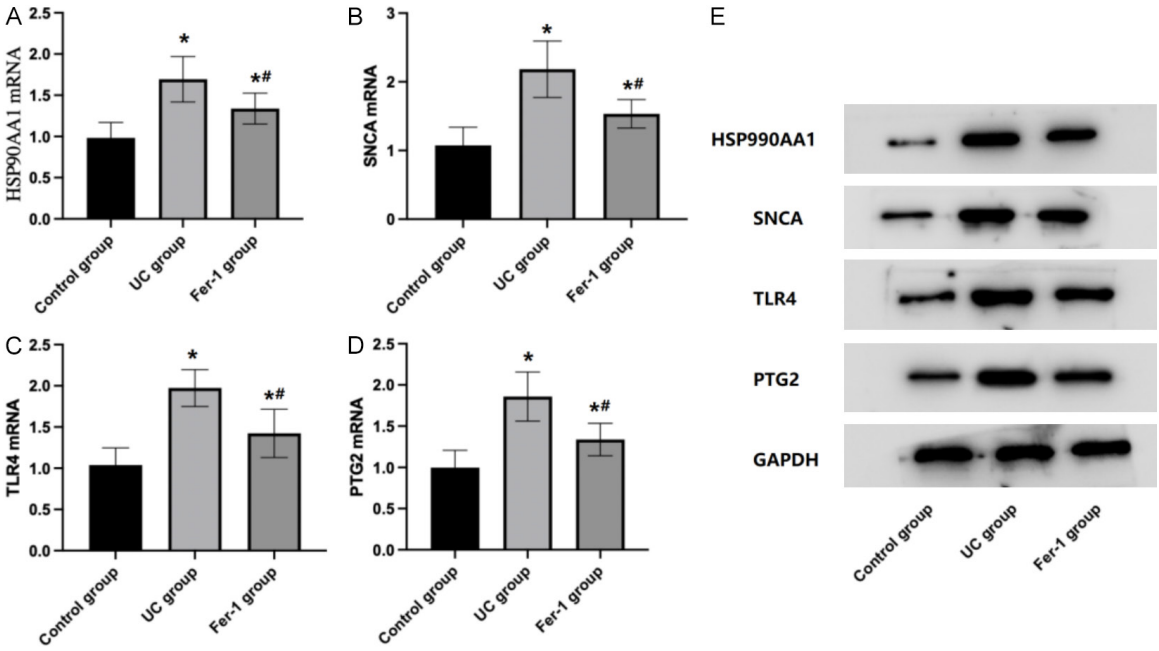

Figure 7. Hub gene expression in colonic tissue of mice in each group. Notes: (A) relative expression of HSP90AA1 mRNA; (B) SNCA mRNA relative expression; (C) TLR4 mRNA relative expression; (D) relative expression of PTG2 mRNA; (E) Western blotting was used to detect the protein expression in the colon tissues of mice in each group. Compared to the control group, *P<0.05; Compared to UC group, #P<0.05.

and amplify inflammatory cascades [22, 23]. It has been proposed that ferroptosis in inflammatory bowel disease may accelerate disease progression by activating immune cells and modulating epithelial cell death. However, the specific ferroptosis network and key regulatory genes in UC remain poorly understood [24, 25]. This study integrated bioinformatics and experimental validation to investigate the expression patterns and molecular mechanisms of the ferroptosis pathway in UC.

In this study, 24 UC-related ferroptosis genes were identified through intersection analysis of the GSE3365 dataset and ferroptosis-related genes, with a focus on four hub genes: HSP90AA1, SNCA, TLR4, and PTGS2. The up-regulation of these genes suggests that ferroptosis may contribute to UC pathogenesis through various biologic processes. HSP90AA1, a member of the heat shock protein family, may regulate the stability of ferroptosis-related proteins under stress, and its overexpression may exacerbate oxidative stress-induced epithelial damage [26-28]. SNCA (α-synuclein), typically associated with neurodegenerative diseases, may participate in ferroptosis in UC by regulating mitochondrial iron metabolism or lipid peroxidation [29, 30]. TLR4, a key receptor of innate immunity, can amplify the inflammatory response through NF-κB and other pathways, creating a positive feedback loop with ferroptosis signaling to promote mucosal barrier disruption [31, 32]. PTGS2 may connect ferroptosis and the inflammatory microenvironment by mediating the synthesis of inflammatory mediators such as prostaglandin E2 [33-35]. Notably, the ferroptosis inhibitor Fer-1 significantly reduced the expression of these hub genes and TNF-α levels, alleviating pathologic damage. These results suggest that ferroptosis may drive inflammation and tissue damage in UC by regulating these hub genes, indicating that targeting the ferroptosis pathway could block the vicious cycle of oxidative stress and inflammation. This offers a novel therapeutic strategy for UC.

However, several limitations should be acknowledged. First, the bioinformatic analysis was based on the public GSE3365 dataset, which has a limited sample size and lacks clinical multicenter validation, potentially affecting the generalizability of the findings. Second, the animal experiments used a DSS-induced UC model, which, although commonly used to simulate

human UC, primarily represents acute inflammation, differing from the chronic inflammation observed in patients. Therefore, further multilevel verification using organoid models or clinical samples is necessary.

In conclusion, this study is the first to reveal that HSP90AA1, SNCA, TLR4, and PTGS2 are key regulatory genes in the ferroptosis pathway in UC, and their abnormal expression may contribute to UC progression through oxidative stress, inflammatory signaling, and lipid metabolism dysregulation. The therapeutic potential of Fer-1 further supports the value of targeting the ferroptosis pathway. However, larger clinical studies, functional experiments, and comprehensive mechanistic investigations are required to clarify the specific targets and regulatory networks of these hub genes, providing a theoretical foundation for developing targeted treatments for UC based on ferroptosis modulation.

Disclosure of conflict of interest

None.

Address correspondence to: Kaiwen Liu, Department of Gastroenterology, Weifang Hospital of Traditional Chinese Medicine, Weifang 261000, Shandong, China. Tel: +86-0536-8590823; E-mail: liukaiw2024@163.com

References

[1] Kucharzik T, Koletzko S, Kannengiesser K and Dignass A. Ulcerative colitis-diagnostic and therapeutic algorithms. Dtsch Arztebl Int 2020; 117: 564-574.

[2] Porter RJ, Kalla R and Ho GT. Ulcerative colitis: recent advances in the understanding of disease pathogenesis. F1000Res 2020; 9: F1000 Faculty Rev-294.

[3] Nakase H, Sato N, Mizuno N and Ikawa Y. The influence of cytokines on the complex pathology of ulcerative colitis. Autoimmun Rev 2022; 21: 103017.

[4] Mourad FH, Hashash JG, Kariyawasam VC and Leong RW. Ulcerative colitis and cytomegalovirus infection: from A to Z. J Crohns Colitis 2020; 14: 1162-1171.

[5] Wangchuk P, Yeshi K and Loukas A. Ulcerative colitis: clinical biomarkers, therapeutic targets, and emerging treatments. Trends Pharmacol Sci 2024; 45: 892-903.

[6] Yao D, Dai W, Dong M, Dai C and Wu S. MUC2 and related bacterial factors: therapeutic targets for ulcerative colitis. EBioMedicine 2021; 74: 103751.

[7] Pabla BS and Schwartz DA. Assessing severity of disease in patients with ulcerative colitis. Gastroenterol Clin North Am 2020; 49: 671-688.

[8] Krugliak Cleveland N, Torres J and Rubin DT. What does disease progression look like in ulcerative colitis, and how might it be prevented? Gastroenterology 2022; 162: 1396-1408.

[9] Peng S, Shen L, Yu X, Zhang L, Xu K, Xia Y, Zha L, Wu J and Luo H. The role of Nrf2 in the pathogenesis and treatment of ulcerative colitis. Front Immunol 2023; 14: 1200111.

[10] Li C, Wu Y, Xie Y, Zhang Y, Jiang S, Wang J, Luo X and Chen Q. Oral manifestations serve as potential signs of ulcerative colitis: a review. Front Immunol 2022; 13: 1013900.

[11] Chen K, Shang S, Yu S, Cui L, Li S and He N. Identification and exploration of pharmacological pyroptosis-related biomarkers of ulcerative colitis. Front Immunol 2022; 13: 998470.

[12] Sun Y, Zhang Z, Zheng CQ and Sang LX. Mucosal lesions of the upper gastrointestinal tract in patients with ulcerative colitis: a review. World J Gastroenterol 2021; 27: 2963-2978.

[13] Long D, Mao C, Huang Y, Xu Y and Zhu Y. Ferroptosis in ulcerative colitis: potential mechanisms and promising therapeutic targets. Biomed Pharmacother 2024; 175: 116722.

[14] Lee KE, Faye AS, Vermeire S and Shen B. Perioperative management of ulcerative colitis: a systematic review. Dis Colon Rectum 2022; 65: S5-S19.

[15] D'Amico F, Magro F, Dignass A, Al Awadhi S, Gutierrez Casbas A, Queiroz NSF, Rydzewska G, Duk Ye B, Ran Z, Hart A, Jairath V, Fiorino G, Peyrin-Biroulet L and Danese S. Practical management of mild-to-moderate ulcerative colitis: an international expert consensus. Expert Rev Gastroenterol Hepatol 2024; 18: 421-430.

[16] Biancone L, Ardizzone S, Armuzzi A, Castiglione F, D'Inca R, Danese S, Daperno M, Gionchetti P, Rizzello F, Scribano ML, Vecchi M and Orlando A. Ustekinumab for treating ulcerative colitis: an expert opinion. Expert Opin Biol Ther 2020; 20: 1321-1329.

[17] Nagaraj T, Shinn J and De Felice K. A practical guide to selecting and using new ulcerative colitis therapies. Curr Opin Gastroenterol 2024; 40: 235-242.

[18] Wang Y, Zhuang H, Jiang XH, Zou RH, Wang HY and Fan ZN. Unveiling the key genes, environmental toxins, and drug exposures in modulating the severity of ulcerative colitis: a comprehensive analysis. Front Immunol 2023; 14: 1162458.

[19] Li W, Zhang L, Xu Q, Yang W, Zhao J, Ren Y, Yu Z and Ma L. Taxifolin alleviates DSS-induced ulcerative colitis by acting on gut microbiome to produce butyric acid. Nutrients 2022; 14: 1069.

[20] Abbas A, Di Fonzo DMP, Wetwittayakhlang P, Al-Jabri R, Lakatos PL and Bessissow T. Management of ulcerative colitis: where are we at and where are we heading? Expert Rev Gastroenterol Hepatol 2024; 18: 567-574.
[21] Zhou Y, Zhu F, Jing D, Wang Q and Zhou G. Ulcerative colitis and thrombocytosis: case report and literature review. Medicine (Baltimore) 2023; 102: e33784.
[22] Zhang M, Zhou J, Wang H, He L, Wang J, Yang X and Zhong X. Exploration of the shared pathways and common biomarker PAN3 in ankylosing spondylitis and ulcerative colitis using integrated bioinformatics analysis. Front Immunol 2023; 14: 1089622.
[23] Marsool MDM, Vora N, Marsool ADM, Pati S, Narreddy M, Patel P, Gadam S and Prajjwal P. Ulcerative colitis: addressing the manifestations, the role of fecal microbiota transplantation as a novel treatment option and other therapeutic updates. Dis Mon 2023; 69: 101606.
[24] De Deo D, Dal Buono A, Gabbiadini R, Spaggiari P, Busacca A, Masoni B, Ferretti S, Bezzio C and Armuzzi A. Management of proctitis in ulcerative colitis and the place of biological therapies. Expert Opin Biol Ther 2024; 24: 443-453.
[25] Stange EF. Steroid-refractory ulcerative colitis: a critical review of national and international guideline recommendations. Z Gastroenterol 2021; 59: 1214-1223.
[26] Dolinger M and Verstockt B. Ulcerative colitis, a transmural disease requiring an accurate IUS assessment in the current treat-to-target era. United European Gastroenterol J 2022; 10: 247-248.
[27] Cheng YW and Fischer M. Fecal Microbiota Transplantation for ulcerative colitis. are we ready for primetime? Gastroenterol Clin North Am 2020; 49: 739-752.
[28] Magro F, Estevinho MM and Feakins R. Inflammation of the appendix in ulcerative colitis - Does it have a predictive value? United European Gastroenterol J 2021; 9: 1107-1108.
[29] Domenech E, Grifols JR, Akbar A and Dignass AU. The Use of granulocyte/monocytapheresis in ulcerative colitis: a practical review from a European perspective. World J Gastroenterol 2021; 27: 908-918.
[30] Levy LC, Coburn ES, Choi S and Holubar SD. The management of the hospitalized ulcerative colitis patient: the medical-surgical conundrum. Curr Opin Gastroenterol 2020; 36: 265-276.
[31] Carvello M, Watfah J and Spinelli A. The management of the hospitalized ulcerative colitis patient, the medical-surgical conundrum. Curr Gastroenterol Rep 2021; 23: 25.
[32] Maio AC, Basile G, Iacopetta D, Catalano A, Ceramella J, Cafaro D, Saturnino C and Sinicropi MS. The significant role of nutraceutical compounds in ulcerative colitis treatment. Curr Med Chem 2022; 29: 4216-4234.
[33] Wang H, He X, Liang S and Chen X. Role of vitamin D in ulcerative colitis: an update on basic research and therapeutic applications. Expert Rev Gastroenterol Hepatol 2022; 16: 251-264.
[34] Kayal M, Meringer H, Martin L and Colombel JF. Systematic review: scores used to predict outcomes in acute severe ulcerative colitis. Aliment Pharmacol Ther 2023; 58: 974-983.
[35] Okabayashi S, Yamazaki H, Matsuoka K, Yamamoto Y and Kobayashi T. Editorial: is older-onset ulcerative colitis more severe or less aggressively managed? Authors' reply. Aliment Pharmacol Ther 2022; 55: 1352-1353.